2022 IMEKO TC-4 International Conference on
Metrology for Archaeology and Cultural Heritage
University of Calabria, Italy, October 19-21, 2022

Simulating weather degradation through heating of a calcarenite from Volterra, Italy: effects on the stone and its consolidation

Andrea Aquino[1, 2], Stefano Pagnotta[2], Marco Lezzerini[2]

[1] *Universität Tübingen, Geo- and environmental research centre, Schnarrenbergstr. 94-96, 72076 Tübingen, Germany, andrea.aquino@uni-tuebingen.de*
[2] *Università di Pisa, Department of Earth Sciences, Via S. Maria 53,56126 Pisa, Italy, stafano.pagnotta@unipi.it, marco.lezzerini@unipi-it*

Abstract – **The "Panchina" stone of Volterra, like that of Livorno, has been, since Etruscan and Roman times, a typical building material widely used in central-southern Tuscany. Here, "Panchina" stone varies in colour from reddish white to yellowish to cerulean, and the grain varies from fine to medium-coarse, depending on the extraction area. In this study, part of a broader study on building stones and their properties, we focus on the chemical-mineralogical and petrophysical characterization of the Volterra "Panchina" stone and its response to thermal stress. After the artificial ageing treatment by heating, various consolidating products were applied to investigate their effectiveness.**

I. INTRODUCTION

This work is part of a broader research framework carried out in recent years at the Department of Earth Sciences of the University of Pisa. These studies are aimed at studying the stones used in historical buildings in Tuscany to understand their characteristics and their response to degradation and consolidation processes [1-6]. In this paper, we focus on one of the two lithotypes constituting the so-called Tuscan 'Pietra Panchina', consisting of two variants, the "Panchina" from Livorno [4, 7-10] e and the "Panchina" from Vollterra, the subject of this study. The "Panchina" stone of Volterra, like that of Livorno, has been, since Etruscan and Roman times, a typical building material in what we now call central southern coastal Tuscany. Evidence of this in Volterra are the ancient Etruscan walls, around 9 km long, the material of which was also studied by Nicolas Steno, who was the first to identify the presence of fossils. The "Panchina" stone in Volterra was also used in the "Porta d'Arco" and in other buildings, such as the Roman pool ("Piscina Romana"). Here, the "Panchina" varies in colour from reddish white to yellowish to cerulean, as does the grain size, depending on where it was quarried, from fine to medium coarse. The fine-grained variety, when polished, takes the commercial name "Pietra Lumachella". In this work, four different samples of Volterra 'Panchina' stone (*latu sensu*) are thermally degraded and analysed.

II. GEOLOGICAL SETTING

The current configuration of Tuscany south of the Arno is the result of a long series of geological events, such as tectonic movements, marine ingressions and transgressions and magmatic activity, which began between the Upper Tortonian and Lower Messinian. In this period, in Tuscany south of the Arno River, a series of sinkings due to tectonic movements led to the formation of lake basins, some of which were later invaded by sea water in the middle to upper Messinian, as evidenced by the development of evaporitic facies (rock salt formations at Saline di Volterra and chalks, containing the famous alabasters, at Volterra and Castellina Marittima). At the end of the Messinian, following the tectonic uplift of much of southern Tuscany, a marine regression occurred. The most important event occurred in the Lower Pliocene: a marine transgression caused by tectonic sinking brought the coastline of the sea to lap the western margins of Monte Albano, the Chianti Mountains and the eastern side of the Val di Chiana. From the resulting new landscape, the little land in front of this new coastline consisted of basins between which emerged some irregular ridges crossed by deep furrows caused by erosion. In these furrows, rainwater flowed towards the new sea carrying the eroded materials. Coarse pebbles and sands were deposited near the outlet into the sea in the form of large conoids, while finer materials were deposited further out, giving rise to sandstones, clays and marly clays. The maximum sea depth was estimated at around 150 metres in front of the Chianti Mountains and greater to the west [11-12]. In this sea, islands emerged, such as that of Poggio del Comune in San Gimignano, surrounded by a shallow bed of gravel consisting of Anfistegina limestone [13]. Other reliefs, such as the Colline Metallifere, were formed by intrusive strains. The Montagnola Senese and Monti Pisani also

emerged from this sea. The present-day Volterra area was located in a shallow part of this sea, and the sedimentation that occurred there gave rise to the following stratigraphic succession, which can be clearly observed today in the Volterra crags [15-16]: a blue clays, sandy clays, clayey sands with clay intercalations, sands and arenaceous limestones: the latter form the 'Bench'. This situation lasted until the Middle Upper Pliocene limit (1.7 m.a.), when a marine regression, caused by general uplift, brought the entire area to the surface.

In the Quaternary, new marine transgressions (Lower Pleistocene) due to tectonic collapses occurred along the Tyrrhenian littoral, while in the Upper Pleistocene (0.125-0.01 m.a.) eustatic marine cycles followed, again along the Tyrrhenian littoral. The latter events are associated with the formation of the 'Panchina' of Livorno and Rosignano.

III. MATHERIALS AND METHODS

For the purposes of this study, we collected four blocks of Volterra stone. Three of these blocks represent the "Panchina" of Volterra, and come from quarries that are no longer cultivated, while the last block represents a variety similar to the "Pietra Forte" sandstone that is locally called "Pietra di Montaione" and is still cultivated. Twelve cubic specimens with dimensions 50*50*50 mm^3 were obtained from these blocks (table 1). For each sample, approximately 250 g of granulate was also obtained, which was then reduced to powder and used for diffractometric and chemical analysis.

Table 1. Samples, lithotype, provenance and number of specimens from each sample.

Sample	Lithotype	Origin	# Specimen
VA	Calcarenite	Volterra (PI)	12
VB	Calcarenite	Volterra (PI)	12
VC	Calcarenite	Volterra (PI)	12
VD	Sandstone	Montaione (FI)	12

The work was divided into three main phases:

1. the chemical, mineralogical and petrographic characterisation of the samples.
2. the petrophysical study.
3. and the artificial weathering phase, followed by consolidation of the samples and analysis of the effects.

Chemical analysis was performed on the powders by X-ray fluorescence [16-17], from which the major and minor elements (Na_2O, MgO, Al_2O_3, SiO_2, P_2O_5, K_2O, CaO, TiO_2, MnO, Fe_2O_3) were determined.

The uncertainty of measurements lies between 4 and 7 wt.% for concentrations <1%, 2-4% for concentrations between 1-10 wt.% and around 1% values >10 wt.% [17-19].

The carbon dioxide content for estimating the calcium carbonate content was measured by gasometry [20]. In particular, the calcite content was calculated with reference to the calibration curve obtained by linking the volume of CO_2 released after acid attack of the rock powder to the amount of pure $CaCO_3$.

X-ray diffractometric analysis, using a Philips PW 1730 diffractometer (λ = 1.5406 Å, angle range 4-66°2θ).

Petrographic analysis was carried out by studying thin sections under transmitted light microscopy.

The physical properties of the samples were then studied according to international standards [21-23]: real (ρ_r) and apparent (ρ_a) density, water absorption coefficient by capillarity, water absorption at atmospheric pressure, total and open porosity and saturation index.

The real density (ρ_r) was determined using a gas pycnometer (Ultrapycnometer 1000 from Quantachrome Corporation) [20]. Measurements were performed on approximately 10 g of ultra-fine-grained powders dried at 105 ± 5 °C for 24 hours under the following experimental conditions: ultra-high purity compressed helium with an outlet pressure of 140 kPa; target pressure, 100 kPa; equilibration time, automatic; purge mode, 3 minutes of continuous flow; maximum number of runs, 6; number of averaged runs, the last three.

Bulk density (ρ_a) was determined from the ratio of dry mass to volume of each sample. The samples were placed in an oven at 60° C until dry weight was reached (i.e. when the difference between two successive weighings at a 24-hour interval is no more than 0.1 per cent of the sample mass). Then the samples were immersed in distilled water according to Leone et al. [20]. The volume of the samples was measured with a hydrostatic balance on water-saturated samples [21].

The water absorption coefficient by capillarity was determined on the same samples used for the determination of bulk density according to EN 1936:2010 [23]. The measurements were carried out after 1, 3, 5, 15, 30, 60, 120, 180, 240, 300, 360, 420, 480, 1440, 2880 minutes.

The determination of water absorption at atmospheric pressure was carried out on the same samples [22].

The total porosity was calculated according to the following formula (1):

$$P\ (\text{vol. \%}) = 100 \cdot (1 - \rho a / \rho r) \quad (1).$$

After the characterisation steps, the samples were artificially degraded by heating in a muffle furnace at different temperatures. 12 specimens for each lithology were divided into three groups: 4 specimens at low temperature 150 °C, 4 samples at 300 °C and 4 samples at 450 °C. The three different artificial degradation temperatures should simulate three different degradation intensities, from mild to strong. After artificial ageing by thermal degradation, the samples were further divided into

two subgroups, one treated with nano silica particles in alcohol solution, and the other with ethyl silicate solution.

The products were applied to each surface of the cubic specimen until complete saturation, which is reached when, 60 minutes after the last application, the surface of the specimen remains visibly covered by residual consolidating material.

The capillarity absorption coefficient was used as a method for determining the degree of rock degradation, but also for evaluating the effectiveness of consolidating products. Therefore, both after artificial weathering and after consolidating treatment, the samples were subjected to a capillarity water absorption cycle.

IV. RESULTS AND DISCUSSION

The mineralogical and petrographic analysis of the samples studied yielded the results summarised in Table 2. In particular, three of the four rock varieties studied are calcarenites (one bio-calcirudite, one calcarenite and one bio-calcarenite), while the last variety, in the sample analysed, represents a quartz sandstone rich in carbonate cement. The colours vary from light brown to beige (bio-calcirudite), reddish grey (calcarenite), yellowish grey (bio-calcarenite) and grey (sandstone). The composition of the various samples is variable, so please refer to Table 2.

Table 2. In the table we report the classification according to Hallsworth & Knox [24], the colour and composition of samples.

Sample	Classif.	Colour	Composition
VA	Bio-calcirudite	Light brown to beige	Bioclasts (55%), quartz (10%), feldspars (10%), lithics (10%, sed. + meta.), sparite (15%)
VB	Calcarenite	Reddish grey	Carb. fragments (40%), quartz (10%), feldspars (10%), bioclasts (5%), carb. cement (15%)
VC	Bio-calcarenite	Yellowish grey	Bioclasts (50%), lithics (20%), quartz (10%), feldspars (5%), carb. cement (15%)
VD	Quartz-sandstone rich in carbonate cement.	Grey	Quartz (30%), bioclasts (30%), lithics (10%), feldspars (5-10%), carb. cement (15%).

As far as the chemical analysis by XRF is concerned, Table 3 shows the main values of the major and minor elements of the analysed samples. In general, the samples show a fair loss on calcination (L.O.I.), between 21 and 32 wt.%, lowest in sandstone and highest in bio-calcarenite.

The CaO values are generally higher (30.8-38.73 wt.%) in the calcarenites (VA, VB and VC), while the VD sandstone sample shows higher values of SiO_2 (41.43 wt.%) than the other samples (24.27-34.94 wt.%). The VD sample also shows higher amounts in other elements (almost twice as much as the other samples): Na_2O (1.28), MgO (1.00), K_2O (1.25), TiO_2 (0.20) and total iron (2.62).

Table 3. Chemical analysis of major and minor components (wt.%). All elements were determined by XRF analysis; L.O.I. obtained by ignition at 980 °C ± 20 °C; CO_2 obtained by gasometer. $Fe_2O_{3\,T}$: total iron as Fe_2O_3 +FeO.

Sample	LOI	Na_2O	MgO	Al_2O_3	SiO_2	P_2O_5	K_2O	CaO	TiO_2	MnO	$Fe_2O_{3\,T}$
VA	28.53	0.67	0.69	3.13	29.69	0.13	0.65	34.71	0.10	0.07	1.63
VB	25.65	0.89	0.83	3.89	34.94	0.11	0.81	30.80	0.13	0.11	1.87
VC	31.65	0.47	0.55	2.28	24.27	0.14	0.54	38.73	0.06	0.09	1.22
VD	21.10	1.28	1.00	6.17	41.43	0.09	1.25	24.77	0.20	0.12	2.62
Mean	*26.73*	*0.83*	*0.77*	*3.87*	*32.58*	*0.12*	*0.81*	*32.25*	*0.12*	*0.10*	*1.83*
St. dev.	*4.49*	*0.35*	*0.19*	*1.67*	*7.33*	*0.02*	*0.31*	*5.95*	*0.06*	*0.02*	*0.59*

Table 4. Averages of the physical parameter values for each sample.

	ρ_r	ρ_a	CI_P	CI_V	P	SI
VA	2.68	2.58	1.2	3.08	3.63	85
VB	2.69	2.51	0.98	2.54	6.8	37
VC	2.70	2.37	1.28	5.62	11.78	48
VD	2.69	2.51	2.42	6.08	6.34	96
Mean	*2.69*	*2.49*	*1.47*	*4.33*	*7.14*	*67*
Dev. St.	*0.01*	*0.09*	*0.65*	*1.78*	*3.40*	*28*

ρ_r: Real density (g/cm^3); ρ_a: Apparent density (g/cm^3); CI_P: Weight imbibition capacity coefficient (%); CI_V: Volume imbibition capacity coefficient; P: porosity (vol. %); SI: saturation index (%).

Moving on to the physical parameters analysed, Table 4 summarises the average values for the individual samples analysed. The bulk density values vary in accordance with the porosity values. The VC sample (bio-calcarenite) shows the highest porosity (11.78 vol. %). The values of the imbibition coefficient (both by weight and volume) are highest for the VD sandstone sample and lowest for the VB calcarenite, ranging from 0.98 to 2.42 CI_P and 2.54-6.08 CI_V.

Table 5. Average values of capillary absorption coefficient (g/m^2 s$^{0.5}$) at 10 minutes for sample and the three temperatures of thermal decay (150, 300 and 450 °C), where applicable.

Sample	Untreated	150 °C	300 °C	450°C	A	B	C
VA	0.08	6.20	6.98	34.66	*1.13*	*5.59*	*4.96*
VB	0.08	5.75	19.58	5.42	*3.41*	*0.94*	*0.28*
VC	0.16	17.46	7.52	8.29	*0.43*	*0.48*	*1.10*
VD	0.09	9.77	19.65	18.58	*2.01*	*1.90*	*0.95*

Untreated: CA values for unweathered samples. A: $CA_{300\,°C}$ / $CA_{150°C}$; B: $CA_{450\,°C}$ / $CA_{150°C}$; A: $CA_{450\,°C}$ / $CA_{300°C}$.

Figure 1 summarises the effects of heat treatment on the samples analysed. For ease of reading, the average values of the four lithotypes (henceforth referred to by the general name "Panchina" calcarenite) are shown. In general, an increase in the amount of water absorbed is observed as the thermal degradation suffered by the rock increases.

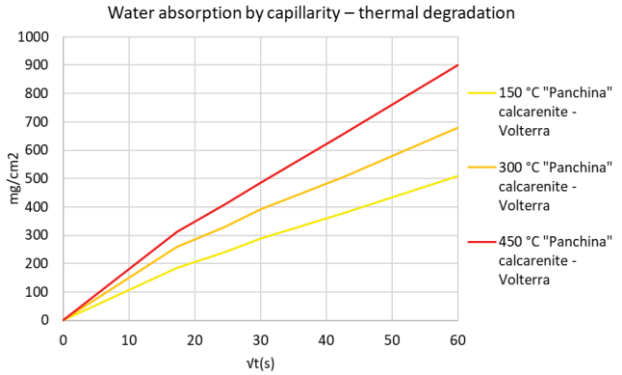

Fig. 1. Average capillary absorption curves for "Panchina" calcarenite from Volterra at different degrees of artificial thermal degradation (150, 300 and 450 °C). The higher the temperature, the higher the amount of water absorbed by the stone.

Table 5 shows the results of the capillary water absorption coefficient of the samples before and after ageing treatment by heating at different temperatures. In all the samples, there is a visible increase in the coefficient value following heat treatment already at 150 °C. In particular, the coefficient value at 150 °C is greater for the VC bio-calcarenite sample, which increases from 0.16 to an impressive 17.46 (g/m^2 s$^{0.5}$). At 300 °C, the greatest increases are recorded by VA and VD, the bio-calcirudite and carbonate-cement quartz sandstone respectively, both with similar values (19.58 e 19.65 g/m^2 s$^{0.5}$). For the last heat treatment at 450°C, the highest values recorded belong to VA (34.66 g/m^2 s$^{0.5}$) and VD (18.58 g/m^2 s$^{0.5}$).

Table 6. Averages of the values of the capillary absorption coefficient (g/m^2 s$^{0.5}$) at 10 minutes.

Spl.	*N*	150 °C			300 °C			450°C		
		b.t.	a.t.	*a.t./b.t.*	b.t.	a.t.	*a.t./b.t.*	b.t.	a.t.	*a.t./b.t.*
Nano-Estel (nano silica solution)										
VA	*0.08*	6.20	2.51	*0.40*	6.98	3.70	*0.53*	34.66	12.71	*0.37*
VB	*0.08*	5.42	3.01	*0.55*	5.75	3.57	*0.62*	19.58	15.36	*0.78*
VC	*0.16*	17.46	9.19	*0.53*	22.94	8.29	*0.36*	36.14	36.14	*1.00*
VD	*0.09*	9.77	3.99	*0.41*	19.65	4.81	*0.24*	18.58	17.46	*0.94*
Estel 1000 (ethyl silicate solution)										
VA	*0.08*	6.20	0.90	*0.14*	6.98	0.85	*0.12*	34.66	1.82	*0.05*
VB	*0.08*	5.42	2.61	*0.48*	5.75	0.89	*0.16*	19.58	2.08	*0.11*
VC	*0.16*	17.46	0.95	*0.05*	22.94	0.97	*0.04*	36.14	3.51	*0.10*
VD	*0.09*	9.77	1.44	*0.15*	19.65	1.44	*0.07*	18.58	1.91	*0.10*

The table shows CA values before artificial weathering (b.t.), after artificial weathering (at 150, 300, 450 °C), and after treatment (a.t.) with Nano-Estel (nano silica solution).

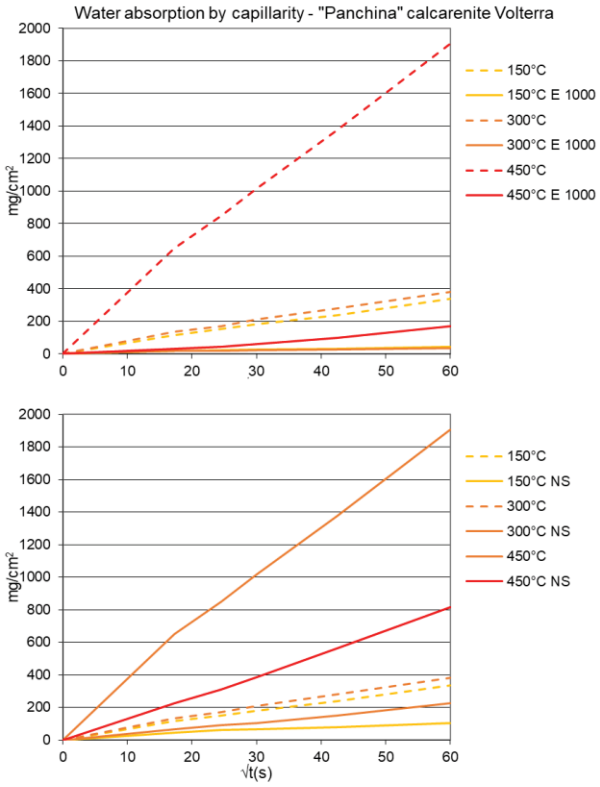

Fig. 2. Comparison of average capillary absorption curves for "Panchina" calcarenite from Volterra at different degrees of artificial thermal degradation (150, 300 and 450 °C) and after treatment with different consolidating materials. E 1000: ethyl silicate; NS: Nano Silica solution. Dotted line: before treatment; plain line: after treatment.

Table 6 and Figure 2 clearly summarise the effects of the application of protective materials such as silica nanoparticle solution and ethyl silicate. Comparing the a.t./b.t. ratio of each sample for the different temperatures, it is clear that the ethyl silicate solution reduces the water ingress of the samples more than the nano silica solution at all temperatures analysed. However, the nano silica particles in solution work in reducing the amount of water absorbed by the samples.

V. CONLUSIONS

The samples studied showed an incremental increase in water content in relation to the increase in temperature to which they were subjected as an artificial ageing treatment. Both consolidants, silica nanoparticle solution and ethyl silicate solution, resulted in a reduction in the capillary absorption coefficient, assumed as a method of evaluating the effectiveness of the consolidants, in the post-heat treatment samples to values close to, and in some cases lower than, those of the pre-treatment rock. Assuming that

less water adsorbed is an indication of better rock condition, in general, silica nanoparticle solution has very good consolidating efficacy, although ethyl silicate is by comparison the best consolidating product. Further studies on the same and other lithologies would be interesting, with particular attention to capillary phenomena.

REFERENCES

[1] Aquino, A., Baglini, P., Pagnotta, S., Tamponi, M., & Lezzerini, M. (2020). Macigno sandstone from Monti d'Oltre Serchio: Chemical, mineralogical, petrographic and physical characterization of a building material. *2020 IMEKO TC-4 International Conference on Metrology for Archaeology and Cultural Heritage*, 50–54.

[2] Aquino, A., Di Petta, C., Pagnotta, S., Tamponi, M., & Lezzerini, M. (2020). Macigno sandstone from Garfagnana and Vellano (north-western Tuscany): Chemical, mineralogical, petrographic and physical characterization of a building material. *2020 IMEKO TC-4 International Conference on Metrology for Archaeology and Cultural Heritage*, 44–49.

[3] Aquino, A., Antola, M., Pacchini, A., Pagnotta, S., & Lezzerini, M. (2020). Thermal decay of monzogranite from Elba Island (western Tuscany, Italy): Properties of an ancient building material. *2020 IMEKO TC-4 International Conference on Metrology for Archaeology and Cultural Heritage*, 38–43.

[4] Aquino, Andrea, Pagnotta, S., Polese, S., Tamponi, M., & Lezzerini, M. (2020). Panchina calcarenite: A building material from tuscany coast. *IOP Conference Series: Earth and Environmental Science*, *609*(1). https://doi.org/10.1088/1755-1315/609/1/012077

[5] Aquino, A., Lezzerini, M. (2019). Performance of consolidants in marble and sandstone from Tuscany: A comparison. *2019 IMEKO TC4 International Conference on Metrology for Archaeology and Cultural Heritage, MetroArchaeo 2019*, 294–298.

[6] Lezzerini, M., Franzini, M., Di Battistini, G., & Zucchi, D. (2008). The «macigno» sandstone from Matraia and Pian di Lanzola quarries (nort h-western Tuscany, Italy). A comparison of physical and mechanical properties. *Atti Della Societa Toscana Di Scienze Naturali, Memorie Serie A*, *113*, 71–79.

[7] Ciampalini, A., Ciulli, L., Sarti, G., & Zanchetta, G. (2006). Nuovi dati geologici del sottosuolo del «Terrazzo DI Livorno». *Atti Della Societa Toscana Di Scienze Naturali, Memorie Serie A*, *111*, 75–82.

[8] Lezzerini, M. (2005). Mappatura delle pietre presenti nella facciata della chiesa di san frediano (Pisa, Italia). *Atti Della Societa Toscana Di Scienze Naturali, Memorie Serie A*, *110*(December), 43–50.

[9] Ramacciotti, M., Spampinato, M., & Lezzerini, M. (2015). The building stones of the apsidal walls of the pisa's cathedral. *Atti Della Societa Toscana Di Scienze Naturali, Memorie Serie A*, *122*. https://doi.org/10.2424/ASTSN.M.2015.20

[10] Sartori, R. (2004). Panchina: materiale lapideo tipico di Livorno e di Volterra. *Bollettino Ingegneri*, *11*, 13–16.

[11] Canuti, P, & Sagri, M. (1974). Ambiente di sedimentazione e provenienza dei clasti nelle anageniti del Verrucano (Appenino settentrionale). *Italian Journal of Geosciences*, *93*(3), 661–704.

[12] Canuti, P., Pranzini, G., & Sestini, G. (1966). Provenienza ed ambiente di sedimentazione dei ciottolami del Pliocene di S. Casciano (Firenze). Arti grafiche Pacini Mariotti.

[13] Fazzuoli, M., Garzonio, C. A., Vannocci, P., & Rodolfi, G. (1982). Lineamenti geolocici e geomorfologici dei dintorni di San Gimignano. *Annali Dell'Istituto Sperimentale per Lo Studio e La Difesa Del Suolo, Firenze*.

[14] Barsotti, G., Federici, P. R., Giannelli, L., Mazzanti, R., & Salvatorini, G. (1974). Studio del Quaternario Livornese, con particolare riferimento alla stratigrafia e alle faune delle formazioni del bacino di carenaggio della Torre del Fanale. *Memorie Della Società Geologica Italiana*, *13*, 425–495.

[15] Bossio, A., Giannelli, L., Mazzanti, R., Mazzei, R., & Salvatorini, G. (1981). Gli strati alti del Messiniano, il passaggio Miocene-Pliocene e la sezione plio-pleistocenica di Nugola nelle colline a NE dei Monti Livornesi. IX Convegno Società Paleontologica Italiana, 55–90.

[16] Franzini, M., Leoni, L., and Saitta, M. (1975). Revisione di una metodologia analitica per fluorescenza-X, basata sulla correzione completa degli effetti di matrice. *Rend. Soc. Ital. di Miner. e Petrol.* 31, 365–378.

[17] Lezzerini, M., Tamponi, M., and Bertoli, M. (2014). Calibration Of XRF data on silicate rocks using chemicals as in-house standards. *Atti della Soc. Toscana di Sci. Nat. Mem. Ser. A* 121, 65–70. doi:10.24.24/ASTSN.M.2014.16.

[18] Tamponi, M., Aquino, A., Pagnotta, S., & Lezzerini, M. (2020). A fast and user-friendly software for quantitative chemical analysis through XRF. *IOP Conference Series: Earth and Environmental Science*, *609*(1), 012058. https://doi.org/10.1088/1755-1315/609/1/012058

[19] Lezzerini, Marco, Tamponi, M., & Bertoli, M. (2013). Reproducibility, precision and trueness of X-RAY fluorescence data for mineralogical and/or petrographic purposes. *Atti Della Societa Toscana Di Scienze Naturali, Memorie Serie A*, *120*(December), 67–73. https://doi.org/10.2424/ASTSN.M.2013.15

[20] Leone, G., Leoni, L., & Sartori, F. (1988). Revisione di un metodo gasometrico per la determinazione di calcite e dolomite. *Atti Della Societa Toscana Di*

Scienze Naturali, Memorie Serie A, *95*, 7–20.
[21] EN 13755. (2009). UNI EN 13755:2009 - Natural stone test methods - Determination of water absorption at atmospheric pressure. *Catalogo UNI*.
[22] EN 1925. (1999). EN 1925:1999 - Natural stone test methods - Determination of water absorption coefficient by capillarity. *British Standards*.
[23] EN 1936. (2010). EN 1936:2010. Natural stone test methods - Determination of real density and apparent density, and of total and open porosity. *British Standards*, *3*.
[24] Hallswort, C. R., and Knox, R. W. O. (1999). *Classification of sediments and sedimentary rocks*. British Geological Survey.